Inverse cascade behavior in freely decaying two-dimensional fluid turbulence

P. D. Mininni[1,2] and A. Pouquet[2]

[1]*Departamento de Física, Facultad de Ciencias Exactas y Naturales, Universidad de Buenos Aires and IFIBA, CONICET, Ciudad Universitaria, 1428 Buenos Aires, Argentina*

[2]*NCAR, P.O. Box 3000, Boulder, Colorado 80307-3000, USA*

(Received 18 May 2011; published 6 March 2013)

We present results from an ensemble of 50 runs of two-dimensional hydrodynamic turbulence with spatial resolution of 2048^2 grid points and from an ensemble of 10 runs with 4096^2 grid points. All runs in each ensemble have random initial conditions with the same initial integral scale, energy, enstrophy, and Reynolds number. When both ensemble and time averaged, an inverse energy cascade behavior is observed, even in the absence of external mechanical forcing: The energy spectrum at scales larger than the characteristic scale of the flow follows a $k^{-5/3}$ law, with negative flux, together with a k^{-3} law at smaller scales, and a positive flux of enstrophy. The source of energy for this behavior comes from the modal energy around the energy-containing scale at $t = 0$. The results shed some light on the connections between decaying and forced turbulence and recent controversies in experimental studies of two-dimensional and magnetohydrodynamic turbulent flows.

DOI: 10.1103/PhysRevE.87.033002 PACS number(s): 47.27.−i, 47.32.C−, 47.65.−d

I. INTRODUCTION

Forced and freely decaying flows are different as far as long-time energetics is concerned. While forced flows can develop both direct and inverse cascades [1,2] (transfer of ideally conserved quantities to smaller or larger scales with constant flux), freely decaying flows can at most display selective decay [3,4] (the faster decay of one invariant relative to another, when the system has two or more ideally conserved quantities and one of them condenses at large scales in the ideal case). These two processes are in practice related: Selective decay results from the transfer of one of the invariants to short wavelengths where the dissipation coefficients are more effective.

For flows with only direct transfer of ideal invariants, e.g., three-dimensional hydrodynamic flows, the distinction between freely decaying and forced flows is not that important. It is well known that if time averaged around the time of maximum dissipation, the spectrum of the ideal invariant develops in the decaying case the same scaling as in forced cases. It is also known that the shape of the spectrum during the decay is preserved under certain conditions [5], resulting in a self-similar decay. The concept of direct cascade is then often applied to these flows indistinctly of the nature of the mechanisms sustaining the turbulence.

However, for flows with inverse transfer of an invariant, the distinction between freely decaying and forced flows remains and dates back to before the introduction of concepts such as selective decay. In two-dimensional hydrodynamic flows, on the one hand, Kraichnan considered the forced case [6] and predicted an inverse cascade of energy with a direct cascade of enstrophy. On the other hand, Batchelor [7] considered the direct transfer of enstrophy in decaying flows, obtaining the long discussed $\sim k^{-1}$ enstrophy spectrum (see, e.g., [8–11]). The reasons for the distinction in this case are clear: As explained by Kraichnan, the possibility of an inverse cascade depends on the relative strengths of the nonlinear interactions between scales. It is natural then to assume that if the input of energy is not sustained for sufficiently long times, the inverse cascade cannot develop and in the flow only the direct cascade, with an increase of the energy-containing scale, will be observed (note that the increase of this scale, however, is distinguishable from the three-dimensional hydrodynamic case).

The main aim of this work is to study under what conditions, in a decaying flow, behavior associated with an inverse cascade (approximately constant negative flux and the corresponding self-similar spectrum with the appropriate scaling law) arises. The motivation to identify such behavior is twofold. On the one hand, phenomena observed in solar wind turbulence and space plasmas are often loosely associated with an inverse cascade of magnetic helicity [12–14]. In many of these cases (e.g., the solar wind) the large-scale dynamics can be well approximated by a decaying magnetohydrodynamic (MHD) flow. Although forced MHD flows develop inverse cascades (of magnetic helicity in three dimensions [15] and the square vector potential in two [16]), based on the previous arguments, results obtained from simulations or theory of forced turbulence do not strictly apply to the decaying case. On the other hand, recent experiments of decaying soap film flows (see [17] for a review) showed in some cases positive third-order velocity structure function [18], inverse energy transfer for scales larger than the injection scale [19], thickness behaving as a passive scalar with Kolmogorov-like scaling [20], and in one case even a disputed $\sim k^{-5/3}$ energy scaling [21], results that are considered indications of inverse cascades in forced two-dimensional flows, but are puzzling in the decaying case.

II. NUMERICAL PROCEDURE

The systems discussed above are complex, with small-scale plasma effects in the case of space flows [22] and with deviations from two dimensionality [23] and finite-size effects [18,24] in the case of soap films. These effects are important to explain the observations (see, e.g., the discussions in [18,20]). With a more humble objective in mind, we take these problems as motivation and focus our attention on differences that may arise in simulations and experiments because of the differences in the procedures followed to obtain turbulent data. To this end, we restrict ourselves to a much simpler system: that

of two-dimensional hydrodynamic flows in the absence of external forces, freely decaying in periodic boxes.

In high-resolution numerical simulations, because of the computational cost, seldom an ensemble of simulations with different initial conditions is done. Instead, only one simulation is done and ergodicity is assumed in order to obtain statistical quantities by averaging in space. Experiments of decaying turbulence are characterized instead by single- or multiple-point measurements of quantities downstream for very long times. The multiple-point measurements can be at similar stages of the evolution or at different stages (e.g., when measuring at different distances downstream from the place where turbulence is generated). The procedure actually results in an average over multiple realizations of decaying flows.

To mimic such a procedure in our simulations, we performed 50 two-dimensional simulations of the Navier-Stokes equations on a regular grid of 2048^2 points. Initial conditions were a random superposition of harmonic modes between wave numbers $k = 18$ and 22, with the spectrum peaking at $k_0 = 20$. Viscosity was $\nu = 2.5 \times 10^{-4}$ in all these runs and the box had length 2π. The initial rms velocity $U_{\rm rms}$ in all runs was 1, corresponding to a turnover time of $\tau_{\rm NL} = L_0/U_{\rm rms} = 2\pi/20 \approx 0.3$ ($L_0 = 2\pi/k_0$). As a result, the runs differed only by their random initial phases.

To study the effect of scale separation between the initial energy-containing scale and the box size, a second set of ten simulations was done with a resolution of 4096^2 grid points. The initial random excitation with $U_{\rm rms} = 1$ was placed between $k = 30$ and 34, with the spectrum peaking at $k_0 = 32$. The initial integral scale of the flow was thus decreased by a factor 1.6 and the initial turnover time was $\tau_{\rm NL} \approx 0.2$. The viscosity in these runs was $\nu = 9.9 \times 10^{-5}$ and as in the previous data set, the runs in this data set differed only in the choice of initial phases.

The equations were integrated up to $t = 6$ using a parallelized pseudospectral code, with the 2/3 rule for dealiasing, and the second-order Runge-Kutta method to evolve in time [25]. Neither friction nor forcing was employed. Note that although the spatial resolutions considered in this study are moderate, the computational cost of computing the whole data set (the fifty 2048^2 runs and the ten 4096^3 runs) is equivalent to that of computing a $16\,384^2$ simulation of two-dimensional turbulence [26].

III. RESULTS

Since the first set has more realizations (50), resulting in more reliable ensemble averages, we focus first on this set and compare at the end with the second data set to identify the effect of increasing resolution. Figure 1 shows the time evolution of the energy spectrum, of the energy flux, and of the enstrophy flux in one of the 2048^3 simulations, i.e., for a single realization. At large wave numbers the energy spectrum develops a direct enstrophy cascade range with an energy spectrum steeper than $\sim k^{-3}$ but shallower than $\sim k^{-4}$. Such spectra have been reported before and for details we refer the reader to the discussion in [11] and references therein. We simply note that, given the separation of scales in this run $k_{\rm max}/k_0 \approx 34$, with $k_{\rm max} = N/3$ the maximum wave number, one does not expect to be able to resolve sufficiently the small-scale range. Recent simulations of forced two-dimensional turbulence, with more scale separation between k_0 and $k_{\rm max}$, indicate a clear $\sim k^{-3}$ energy scaling at small

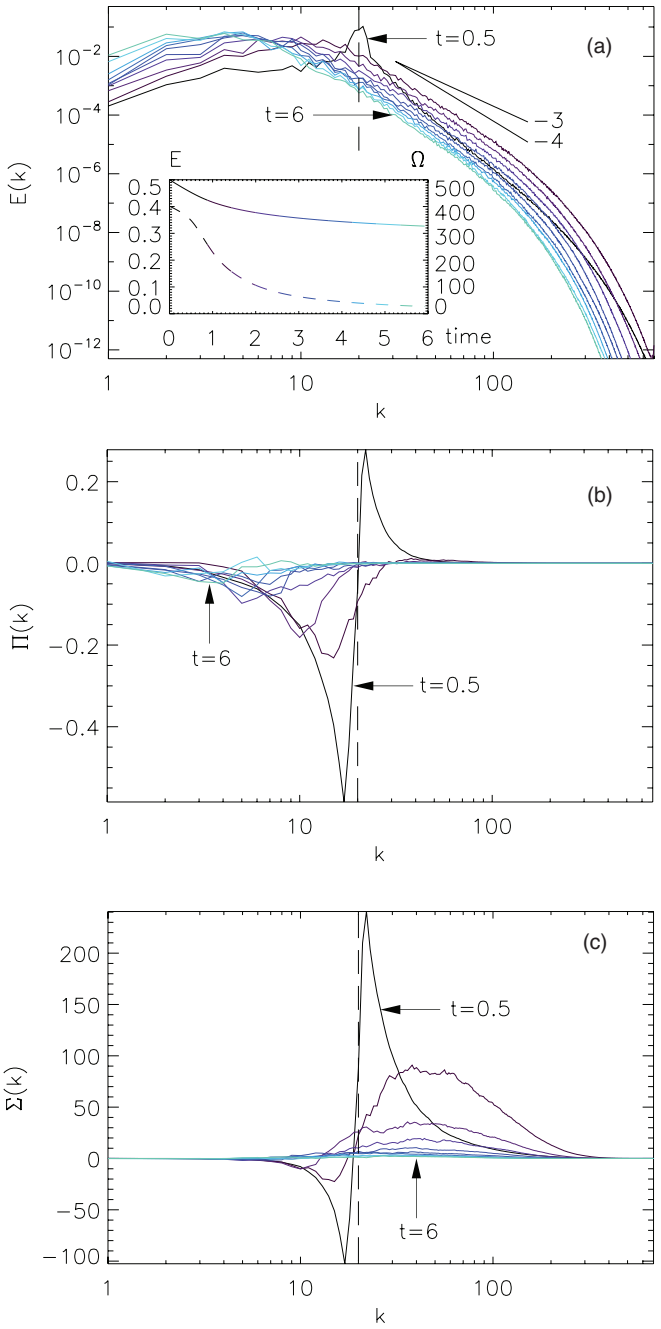

FIG. 1. (Color online) Time evolution of the (a) energy spectrum, (b) energy flux, and (c) enstrophy flux in a single 2048^3 simulation from $t = 0.5$ (black line) to $t = 6$ (light gray or light blue line). Slopes in the energy spectrum are indicated as references. The curves corresponding to $t = 0.5$ and 6 are indicated in all panels by arrows and the vertical dashed lines indicate the initial energy containing wave number k_0. In (b) and (c), note the displacement to smaller wave numbers of the minimum of energy flux and to larger wave numbers of the maximum of enstrophy flux. The inset in (a) shows the time evolution of the energy (solid line) and of the enstrophy (dashed line) in this run, with the color changing with time following the colors used for the different curves in the spectrum and fluxes.

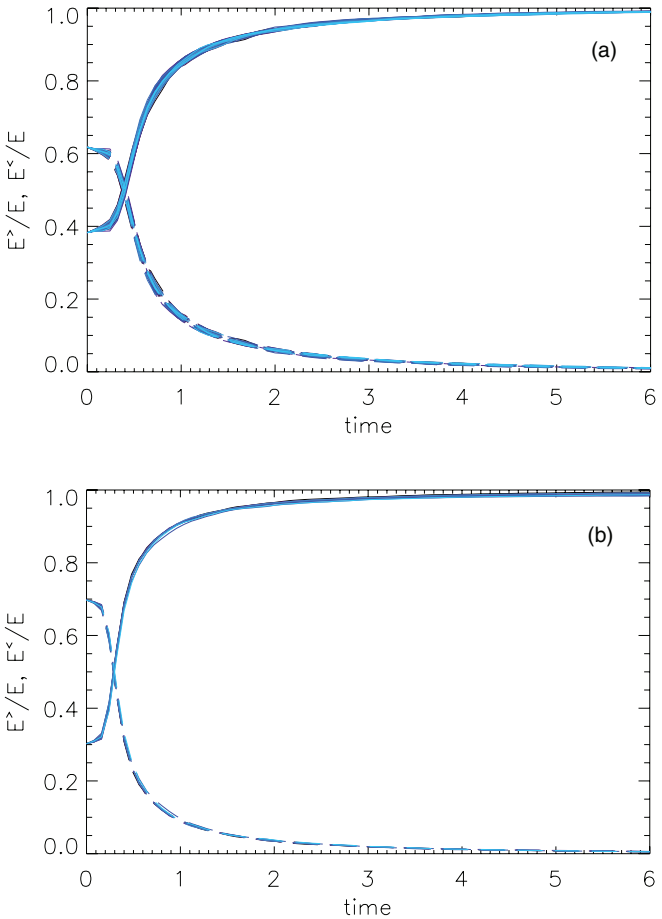

FIG. 2. (Color online) Time evolution of $E^{<}/E$ (solid line) and $E^{>}/E$ (dashed line) (ratio of the energy at large and small scales, respectively, to the total energy) as a function of time for all runs in the set of simulations with (a) 2048^2 grid points and (b) 4096^2 grid points.

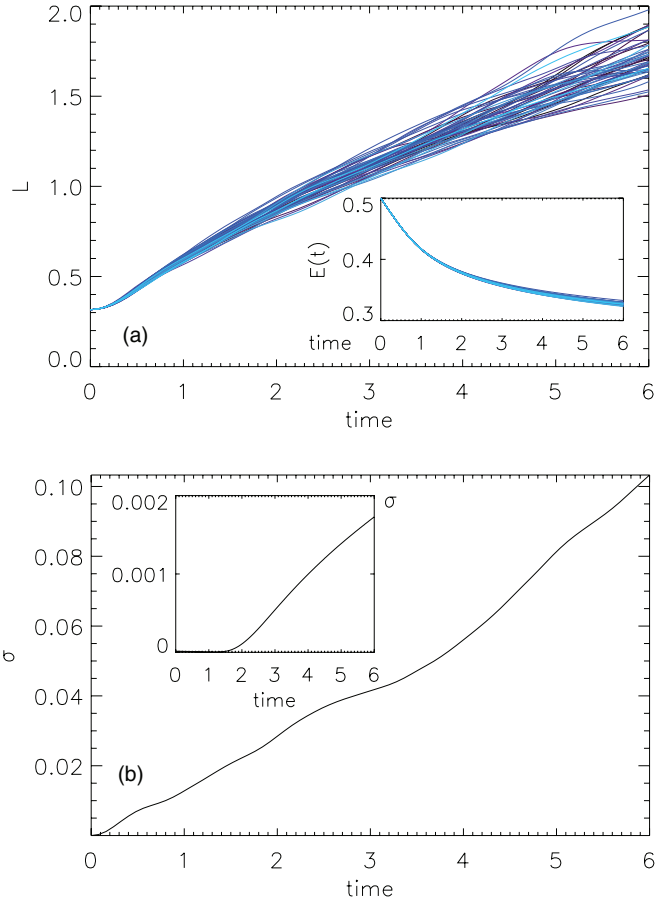

FIG. 3. (Color online) (a) Time evolution of the integral scale for all the 2048^2 runs; note the dispersion around the mean evolution. The inset shows the time evolution of the energy for all runs, which are very close. (b) Time evolution of the standard deviation σ in the integral scale of all the 2048^2 runs. The inset shows the standard deviation in the energy in all the 2048^2 runs as a function of time.

scales [27], as expected from Batchelor phenomenology (see also [1,24]). Since this is not the main purpose of this paper, we just want to stress that the resulting inertial range is compatible with moderate Reynolds number runs done in the past.

We are interested here instead in the spectrum at wave numbers smaller than the initial energy-containing wave number k_0. At those wave numbers, the peak of energy moves towards smaller wave numbers as time evolves, leaving to its left an energy spectrum again consistent with the direct enstrophy range. The fluxes are in agreement with this picture: The energy flux has a negative peak that moves towards smaller wave numbers with time, but has no identifiable range with approximate constancy. In contrast, the enstrophy flux develops a wide quasiconstant range starting at $t \approx 1$ and as its amplitude decreases with time, this range can still be identified.

The displacement of the peak of the energy spectrum towards smaller wave numbers can be associated with the well-known increase of the flow integral length L as the energy decays. However, it does not automatically follow that the increase of L is the sign of an inverse cascade. Indeed, the integral length scale also grows in a three-dimensional flow as is well known, due to the preservation of large-scale correlations in the von Kármán–Howarth equation [28,29] with spectra $\sim k^{+n}$, with n equal to either 2 or 4, and also due to the eddy noise created by the beating of two interacting small scales. As the peak of the energy spectrum in three-dimensional turbulence moves to larger scales, the amplitude of the peak decreases, being modulated by the $\sim k^{+n}$ spectra. In contrast, the growth of the integral scale in an inverse cascade is accompanied by another phenomenon, that of the growth of energy at large scales.

Unlike freely decaying three-dimensional turbulence, the energy at large scales in the two-dimensional runs increases substantially as time evolves. This can be seen in Fig. 2, which shows the energy at large scales (wave numbers smaller than k_0)

$$E^{<} = \sum_{k=1}^{k_0-1} E(k) \tag{1}$$

and the energy at small scales (wave numbers larger than k_0)

$$E^{>} = \sum_{k=k_0}^{k_{\max}} E(k), \tag{2}$$

normalized by the total energy as a function of time. In both runs, the small-scale energy decreases rapidly, while the large-scale energy grows. When not normalized by the total energy, $E^<$ still grows and then slowly decays as a result of viscous forces (with a slower decay in the 4096^2 run). In the absence of a transfer of energy towards large scales (i.e., without a negative energy flux), $E^<$ would only decrease in time.

The time evolution of the integral scale for all 2048^2 runs is shown in Fig. 3. In spite of the fact that the runs differ only by their initial phases, there is a large dispersion in the time evolution of L, more so than for the energy [see the inset of Fig. 3(a)]. The actual dispersion in the evolution of L and E in the different runs is also quantified in Fig. 3(b), by means of the standard deviation σ. For both quantities, σ first grows exponentially (at very early times) and later seems to follow an approximate linear growth with time. From pioneering works on the predictability of two-dimensional turbulence [30–32] (see also [33,34] for recent studies), we can expect differences in the initial conditions to grow first at the initial energy-containing scale (resulting in the early exponential phase) and later to propagate towards larger scales if an inverse cascade develops (see [34] for a numerical study). In that regime, the time it takes for the differences to propagate is that of the turnover time, which if a Kolmogorov spectrum is assumed, results in linear growth of the error with time [30,34]. Note that the integral scale L is obtained from the energy spectrum weighting the most energetic wave numbers and as such more deviation can be expected than in the case of the total energy.

Although the standard deviation observed in Fig. 3 can be expected in an ensemble, numerical simulations often deal with only one of the realizations. What are the implications of the dispersion in the integral length (and energy) in the different simulations at a given time? Figure 4 shows the energy spectrum at $t = 1.5$ and 6 for ten randomly picked

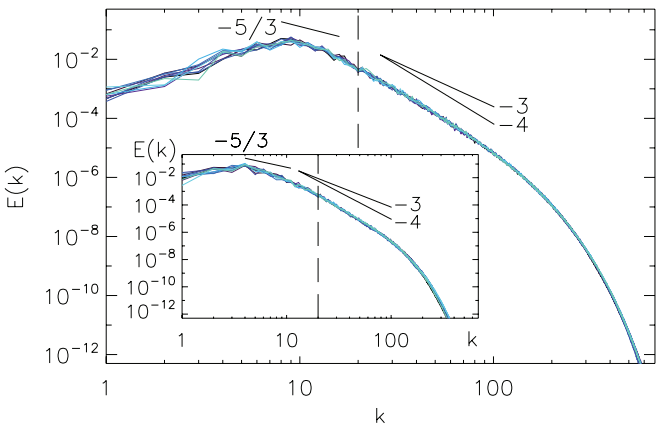

FIG. 4. (Color online) Energy spectra for ten 2048^2 runs at $t = 1.5$ (no averaging performed here). Slopes are indicated as references. The vertical dashed line corresponds to the initial energy-containing wave number k_0. The inset shows the same ten spectra at $t = 6$. Note that the large-scale spectra look like $\sim k$, which could be interpreted as eddy noise in two dimensions (see [35]). However, unlike three-dimensional turbulence, the amplitude of the peak of the energy spectrum is larger than its initial value (at $t = 0$) at the same wave number.

2048^2 runs. At $t = 1.5$, a narrow range seems to emerge at large scales, with a slope shallower than $\sim k^{-3}$, between the energy-containing scale and the enstrophy range. Exploration of the energy flux (not shown) indicates that its ensemble average may display a short range with approximate constancy. Moreover, at later times (see, e.g., the inset in Fig. 4), this shallower range in the energy spectrum increases in width and moves to smaller wave numbers.

Based on this result, we show in Fig. 5 the time- and ensemble-averaged energy spectrum, energy flux, and enstrophy flux for the set of simulations with 2048^2 grid points.

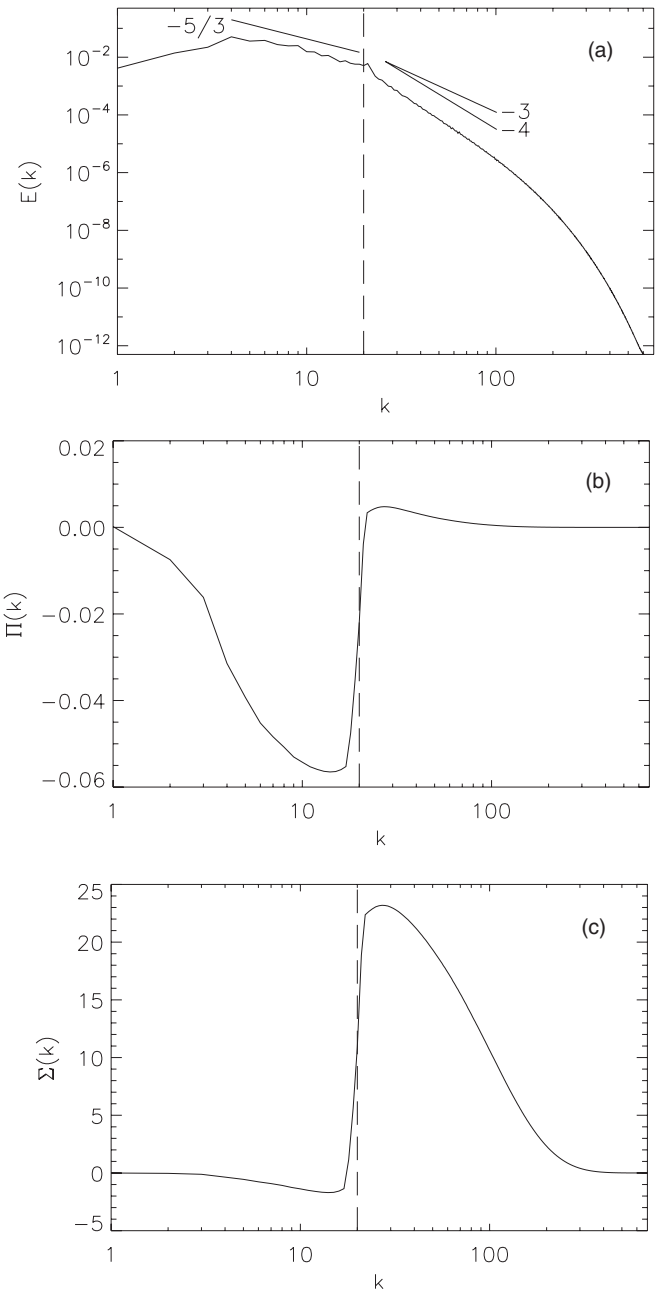

FIG. 5. (a) Time- and ensemble-averaged energy spectrum, (b) energy flux, and (c) enstrophy flux over the fifty 2048^2 simulations and from $t = 0.5$ to 6. Slopes in (a) are indicated as references. The vertical dashed lines correspond to the initial energy-containing wave number k_0.

The average is computed over the 50 simulations and from $t = 0.5$ to 6. Now a wide $\sim k^{-5/3}$ spectrum clearly emerges at wave numbers smaller than the initial energy-containing wave number, followed by the enstrophy range at larger wave numbers. The energy flux now also displays a wider range in which it remains negative and non-negligible (note that a negative energy flux corresponds to a positive third-order longitudinal velocity structure function). Moreover, a clear distinction can be made between the range with negative energy flux and negligible enstrophy flux and the range with positive enstrophy flux and negligible energy flux. Finally, note that, dimensionally, $\Sigma \sim k_0^2|\Pi|$, which is well verified by the data; in other words, the observed energy and enstrophy fluxes (to large and small scales, respectively) are comparable when properly normalized using the characteristic length scale of the flow at $t = 0$.

The same time and ensemble averages are shown in Fig. 6 for the ten runs with 4096^2 grid points (as the scale separation between initial perturbation and dissipation scale is roughly the same in this set of runs as in the runs with 2048^2 points, the flux of enstrophy is similar to the one in Fig. 5 and is not shown). The larger scale separation at large scales allows for the development of a slightly wider $\sim k^{-5/3}$ spectrum.

The results in Figs. 5 and 6 indicate that after time and ensemble averaging, well-known features of the inverse energy cascade in forced two-dimensional hydrodynamic turbulence

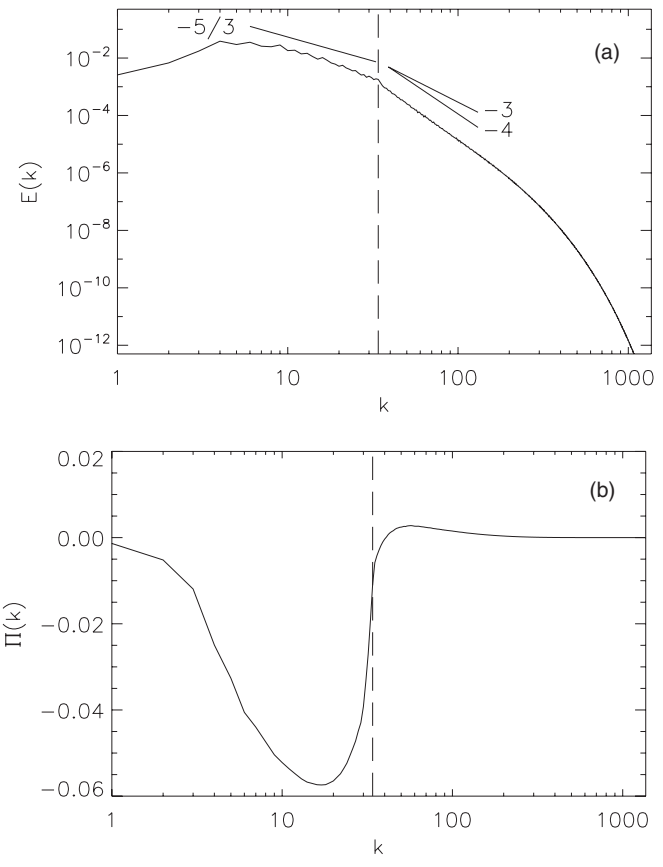

FIG. 6. (a) Time- and ensemble-averaged energy spectrum and (b) energy flux over the ten 4096^2 simulations and from $t = 0.5$ to 6. Slopes in (a) are indicated as references. The vertical dashed lines correspond to the initial energy-containing wave number k_0.

can be identified in decaying flows. The $\sim k^{-5/3}$ energy spectrum emerges as an envelope to the evolution of the large-scale energy spectrum, which instantaneously and for each run only shows a clear direct enstrophy range. It is interesting to point out that time and ensemble averages of freely decaying two-dimensional turbulence were used before (see [36]). There a spectrum for the enstrophy $\sim k$ [i.e., $E(k) \sim k^{-1}$] was observed at scales larger than the initial energy-containing scale. Although this indicates a growth of energy at large scales, the spectrum is shallower than the one reported here, probably because in that study much later times were considered when studying the decay (over 100 turnover times).

IV. DISCUSSION

Experiments, as well as observations of space flows, do not allow for such a tight control of initial rms velocities and initial injection scales as in the present simulations, which kept these quantities the same in all the initial conditions. It can be conceived that as these initial quantities are allowed to vary within a certain percentage, the dispersion of the integral scale and of the energy at a later time during the decay will become larger. This, in a much larger ensemble of runs, may allow for a $\sim k^{-5/3}$ energy spectrum to arise without time averaging, as each realization at a given time may correspond to different stages of the decay.

Although in the applications discussed in the Introduction other effects may be playing a role to explain the observations, it is remarkable that a link between the behavior of forced and decaying flows was missed for such a long time. We offer a possible explanation for this. In a time when computers allow us to study larger and larger Reynolds numbers and many studies are focused on achieving the largest possible Reynolds number, the present study points to the need to use computer power also to perform longer runs and ensembles of runs (as routinely done in climate studies) to be able to compare on an equal footing with experiments and theory and to validate some of the usual assumptions in the field, such as ergodicity (in the sense that time and spatial averages can be seamlessly interchanged when comparing experiments and simulations) and, as was our focus here, distinctions between forced and decaying flows.

It is worth recalling in this context that the statistical mechanics of ideal (unforced) flows, which have a signature of a condensate of energy at large scales, were the basis on which Kraichnan's conjecture of the inverse cascade was made, so it is not necessarily surprising to find such a behavior in the decay run as well since it stems from the nature of two-dimensional nonlinear triadic interactions and the constraints of conservation. Indeed, the triads responsible for the inverse cascade of energy are present in freely decaying flows and whether or not they can act is a problem of energetics (i.e., whether their amplitude is large enough and can be sustained for sufficiently long times). It is therefore important to point out that it has been shown that a $\sim k^{-5/3}$ energy spectrum is the minimally steep spectrum that is able to support an inverse cascade of energy [37] (i.e., a shallower spectrum cannot sustain the inverse cascade). The behavior observed in these freely decaying simulations can thus only be observed

for a certain period of time, as the energy is spread over more wave numbers and the inverse energy flux decreases with time (see Fig. 1). In the forced case, the external forcing supplies the required energy to sustain the flux in time and to give a persistent $\sim k^{-5/3}$ energy spectrum.

Interestingly, recently other problems were found in fluid dynamics in which particular triads allowed for transient or sustained inverse cascades. Such is the case, e.g., of three-dimensional helical flows restricted to triadic interactions with only the same sign of helicity in all interacting modes [38]. In this latter case, the inverse cascade was sustained in time instead of being transient, as it resulted from an artificial amplification in the simulation of particular triads.

Other similarities between decaying flows and the forced Kraichnan inverse energy cascade may arise and are left for future work. In particular, the intermittency of the large scales, the effect on the structures, and the equivalent behavior in MHD can be studied and may be of interest for many applications.

ACKNOWLEDGMENTS

Computer time was provided by the National Center for Atmospheric Research, which is sponsored by the National Science Foundation. The authors acknowledge support from NSF CMG Grant No. 1025183 and P.D.M. acknowledges support from PICT Grants No. 2011-1529 and No. 2011-1626.

[1] R. Kraichnan and D. Montgomery, Rep. Prog. Phys. **43**, 547 (1980).
[2] U. Frisch, *Turbulence: The Legacy of A.N. Kolmogorov* (Cambridge University Press, Cambridge, 1995).
[3] W. H. Matthaeus and D. Montgomery, Ann. N.Y. Acad. Sci. **357**, 203 (1980).
[4] A. C. Ting, W. H. Matthaeus, and D. Montgomery, Phys. Fluids **29**, 3261 (1986).
[5] A. N. Kolmogorov, Dokl. Akad. Nauk. SSSR **31**, 538 (1941).
[6] R. Kraichnan, Phys. Fluids **10**, 1417 (1967).
[7] G. K. Batchelor, Phys. Fluids **12**, II-233 (1969).
[8] A. Bracco, J. C. McWilliams, G. Murante, A. Provenzale, and J. B. Weiss, Phys. Fluids **12**, 2931 (2000).
[9] P. Dmitruk and D. C. Montgomery, Phys. Fluids **17**, 035114 (2005).
[10] D. G. Dritschel, C. V. Tran, and R. K. Scott, J. Fluid Mech. **591**, 379 (2007).
[11] E. Lindborg and A. Vallgren, Phys. Fluids **22**, 091704 (2010).
[12] M. Christensson, M. Hindmarsh, and A. Brandenburg, Phys. Rev. E **64**, 056405 (2001).
[13] P. Démoulin and E. Pariat, Adv. Space Res. **43**, 1013 (2009).
[14] P. Démoulin and S. Dasso, Astron. Astrophys. **498**, 551 (2009).
[15] A. Pouquet, U. Frisch, and J. Léorat, J. Fluid Mech. **77**, 321 (1976).
[16] A. Pouquet, J. Fluid Mech. **88**, 1 (1978).
[17] H. Kellay and W. I. Goldburg, Rep. Prog. Phys. **64**, 845 (2002).
[18] A. Belmonte, W. I. Goldburg, H. Kellay, M. A. Rutgers, B. Martin, and X. L. Wu, Phys. Fluids **11**, 1196 (1999).
[19] M. K. Rivera, W. B. Daniel, S. Y. Chen, and R. E. Ecke, Phys. Rev. Lett. **90**, 104502 (2003).
[20] O. Greffier, Y. Amarouchene, and H. Kellay, Phys. Rev. Lett. **88**, 194101 (2002).
[21] M. Gharib and P. Derango, Physica D **37**, 406 (1989).
[22] P. D. Mininni, D. O. Gómez, and S. M. Mahajan, Astrophys. J. **584**, 1120 (2003).
[23] Y. Couder, J.-M. Chomaz, and M. Rabaud, Physica D **37**, 384 (1989).
[24] H. J. H. Clercx and G. J. F. van Heijst, Phys. Rev. Lett. **85**, 306 (2000).
[25] D. O. Gómez, P. D. Mininni, and P. Dmitruk, Phys. Scr. **T116**, 123 (2005).
[26] G. Boffetta and R. E. Ecke, Annu. Rev. Fluid Mech. **44**, 427 (2011).
[27] A. Vallgren and E. Lindborg, J. Fluid Mech. **671**, 168 (2011).
[28] P. A. Davidson, *An Introduction to Magnetohydrodynamics* (Cambridge University Press, Cambridge, 2001).
[29] T. Ishida, P. A. Davidson, and Y. Kaneda, J. Fluid Mech. **564**, 455 (2006).
[30] E. N. Lorenz, Tellus **21**, 289 (1969).
[31] C. E. Leith, J. Atmos. Sci. **28**, 145 (1971).
[32] C. E. Leith and R. H. Kraichnan, J. Atmos. Sci. **29**, 1041 (1972).
[33] G. Boffetta, A. Celani, A. Crisanti, and A. Vulpiani, Phys. Fluids **9**, 724 (1997).
[34] G. Boffetta and S. Musacchio, Phys. Fluids **13**, 1060 (2001).
[35] S. Fox and P. A. Davidson, Phys. Fluids **21**, 125102 (2009).
[36] D. G. Dritschel, R. K. Scott, C. Macaskill, G. A. Gottwald, and C. V. Tran, Phys. Rev. Lett. **101**, 094501 (2008).
[37] C. V. Tran, Phys. Fluids **19**, 108109 (2007).
[38] L. Biferale, S. Musacchio, and F. Toschi, Phys. Rev. Lett. **108**, 164501 (2012).